Speckle Statistics in Adaptive Beamforming

Johan-Fredrik Synnevåg Carl-Inge Colombo Nilsen Sverre Holm

Department of Informatics, University of Oslo
P.O. Box 1080, N-0316 Oslo, Norway

Abstract— **We have examined the statistics of the speckle patterns in images formed using delay-and-sum and minimum variance beamforming. We show how the estimate of the spatial covariance matrix used in the latter beamformer affects the speckle patterns. By using purely spatial averaging in the estimate the speckle statistics are quite different from delay-and-sum: Areas that are apparently homogeneous in delay-and-sum images appear as a collection of point scatterers in the minimum variance images, reducing the overall brightness of the speckle. We show that temporal averaging reduces this effect without compromising the improved spatial resolution offered by the minimum variance beamformer. Results from both simulations and experimental RF data are shown.**

I. Introduction

A number of authors have applied adaptive beamforming to medical ultrasound imaging [1], [2], [3], [4], [5], [6]. Superior resolution has been demonstrated on point scatterers, but little attention has been paid to the effect on so called "speckle", which is the grainy appearance of homogeneous areas in ultrasound images. Speckle in ultrasound B-mode images has been researched since Burckhardt's initial paper in 1978 [7]. This research has resulted in a number of theories seeking to describe and explain the statistical properties of speckle, as well as many suggested methods for speckle reduction.

In this paper we investigate the difference in speckle statistics on images formed by delay-and-sum (DAS) and minimum variance (MV) beamformers. In particular, we examine the effects of temporal and spatial averaging on system resolution and speckle statistics of the MV beamformer. Fig. 1, which shows images of a heart phantom formed by DAS and MV, demonstrates the starting point of our investigation: while giving better edge definition, the MV beamformer in Fig. 1(b) gives the impression of point scatterers in homogeneous tissue. These structures appear more homogeneous and brighter in Fig. 1(a) which shows the image formed using DAS. Hence, the MV image displays a lower contrast.

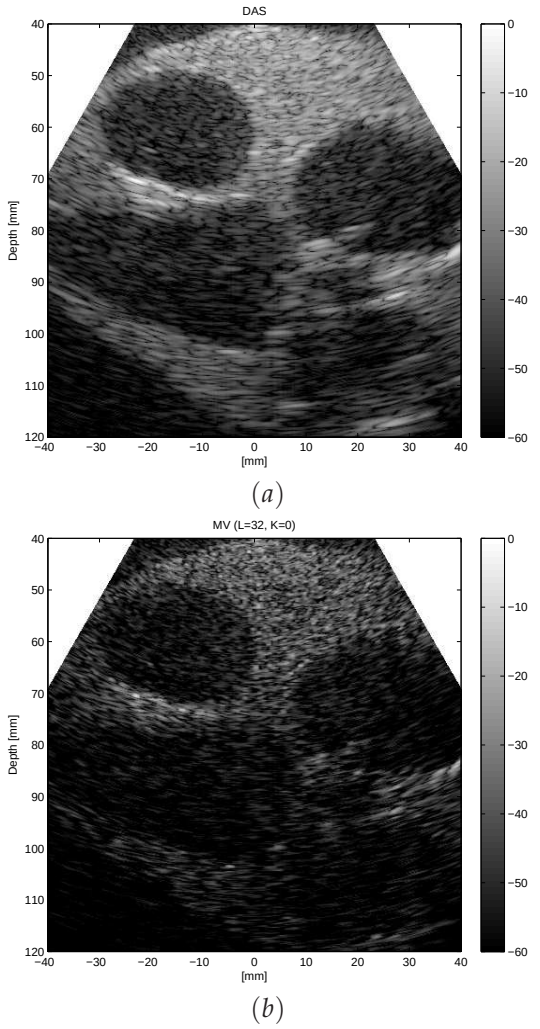

Fig. 1. Heart phantom imaged by a 15.4 mm, 64 element 3.33 MHz transducer. (a) DAS and (b) MV ($L = 32$, $K = 0$). Transmit focus was 60 mm.

II. Methods

A. The MV beamformer

We assume an M element transducer in which $x_m[n]$ is the sampled output from element m. The output of a general beamformer operating on these measurements can be described as:

$$z[n] = \sum_{m=0}^{M-1} w_m[n] x_m[n - \Delta_m] = \mathbf{w}^H[n]\mathbf{X}[n], \qquad (1)$$

where $w_m[n]$ is a (complex) weight, Δ_m is a delay applied to channel m to focus at a specific point in the image, $\mathbf{w}^H[n] = \{w_0[n] \cdots w_{M-1}[n]\}$ and $\mathbf{X}[n] = \{x_0[n - \Delta_0] \cdots x_{M-1}[n - \Delta_{M-1}]\}^T$. For a DAS beam-

former the weights, $\mathbf{w}[n]$, are predetermined with the objective of minimizing sidelobes while keeping a narrow mainlobe. For the MV beamformer, $\mathbf{w}[n]$ is calculated from the recorded data by minimizing the variance of $z[n]$ while maintaining unit gain at the focal point. The analytical solution to this problem is given by [8]:

$$\mathbf{w}[n] = \frac{\mathbf{R}^{-1}[n]\mathbf{a}}{\mathbf{a}^H\mathbf{R}^{-1}[n]\mathbf{a}}, \tag{2}$$

where $\mathbf{R}[n]$ is the spatial covariance matrix, and $\mathbf{a}$ is the steering vector. Since the signals in $\mathbf{X}[n]$ have been delayed, $\mathbf{a}$ is a vector of ones.

In practice $\mathbf{R}[n]$ must be estimated, either by averaging in the temporal domain, the spatial domain, or both. Averaging in the spatial domain is done by dividing the transducer into (overlapping) subarrays and averaging the spatial covariance matrices of each subarray. The general covariance matrix estimate averaged over $2K+1$ temporal samples and $M-L+1$ subarrays of length L is given by:

$$\hat{\mathbf{R}}[n] = \frac{1}{(2K+1)(M-L+1)} \sum_{k=-K}^{K} \sum_{l=0}^{M-L} \mathbf{X}_l[n-k]\mathbf{X}_l^H[n-k], \tag{3}$$

where $\mathbf{X}_l[n] = \{x_l[n-\Delta_l] \cdots x_{l+L-1}[n-\Delta_{l+L-1}]\}^T$. The subarray length, L, determines the degrees of freedom in the MV estimate. A smaller L gives a more robust estimate at the expense of resolution. The MV amplitude estimate is found by averaging the output of each subarray beamformer:

$$z_{MV}[n] = \frac{1}{M-L+1} \sum_{l=0}^{M-L} \mathbf{w}^H[n]\mathbf{X}_l[n]. \tag{4}$$

B. Speckle Statistics

As in optics, speckle is described as the result of scattering a transmitted signal by a large number of subwavelength sized particles that are densely distributed in space with random distances following a uniform probability density. "Densely" is meant with respect to the resolution cell size of the imaging system in question. The distribution of particles is considered spatially uncorrelated. When adding the phase shifted contributions from all these scatterers, the result is a signal with a Rayleigh distributed magnitude.

The spatial correlation of the resulting image does not reflect that of the original, uncorrelated particle distribution, but rather gives the impression of the existence of structures in the homogeneous tissue. Research suggests that these patterns reflect the resolution properties of the imaging system itself and no specific properties of the tissue (e.g. [9]). This means that the parameters of the intensity distribution are affected when changing the aperture by for instance increasing the array size or applying a weighting function. As adaptive beamformers like the MV beamformer apply time-varying weights that are calculated using the (estimated) spatial covariance matrix of the received signal, this will affect speckle statistics differently than DAS beamformers with constant weights. A clear difference is that the "resolution" of a MV beamformer is not fixed; it cannot be connected to the properties of a static beampattern like in the case of DAS. Instead it depends, for instance, on the accuracy of the covariance matrix estimate.

III. Results

A. Simulations

We simulated two phantoms using Field II [10]: To estimate the speckle statistics obtained by the DAS and MV beamformers we simulated 100,000 point scatterers randomly distributed within an area of 20x20x20 mm. All reflection coefficients of the scatterers were set equal. In the second phantom we used the same distribution of point scatterers, but added four strong reflectors, leading to speckle images with four distinct points.

We simulated an 18.5 mm, 96 element, 4 MHz transducer. All transmitter and receiver combinations were simulated, allowing dynamic focus on both transmission and reception. We synthesized dynamic transmit focus by combining appropriately delayed receiver channels from each transmit element. The new set of receiver channels were then dynamically delayed. Delays were implemented by upsampling and selecting the sample closest to the theoretically predicted delay. For the DAS beamformer, the receiver channels were then summed. For MV, the aperture weights were calculated and applied.

B. Speckle patterns

Fig. 2 shows images of the four point scatterers surrounded by speckle formed by DAS and MV for different subarray lengths. All MV results use $K = 0$, corresponding to no temporal averaging. We see that as L increases the point scatterers are better defined. We also see that the intensity of the speckle is reduced when the subarray length increases. For $L = 48$ the speckle grains seem to be resolved into individual point scatterers. This may be an undesirable effect in medical ultrasound imaging where speckle regions are important for the image formation.

To investigate the statistics of the speckle in Fig. 2 we used the simulation of the phantom without the four strong reflectors. Fig. 3 shows the magnitude distributions for the images consisting of pure speckle for DAS and MV with different subarray lengths. We see that the distributions resemble Rayleigh distributions for all beamformers, but with different average magnitude and variance. For the "one-sample" ($K = 0$) MV beamformers the average magnitude is reduced as L increases.

Fig. 4 shows corresponding images as in Fig. 2, but with different amount of temporal averaging for the MV beamformer. Fig. 4(a) shows DAS and Fig. 4(b)-(d)

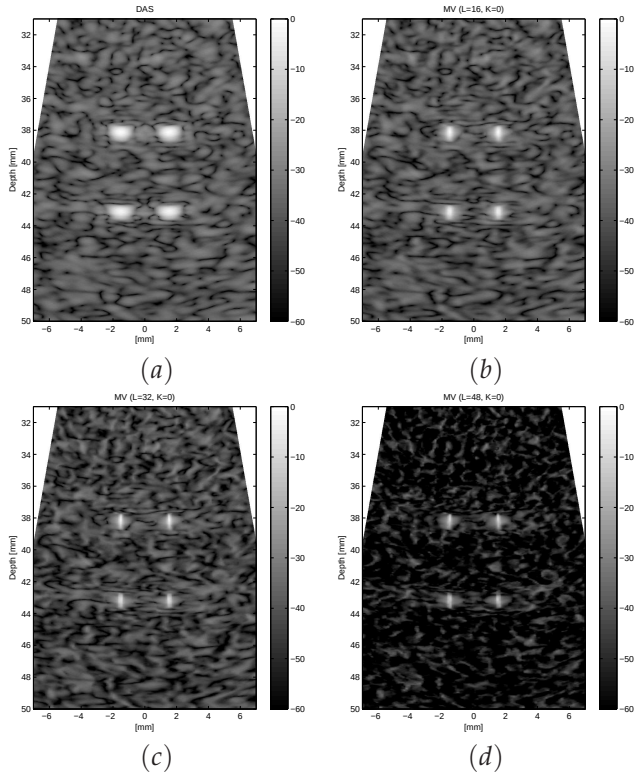

Fig. 2. Images of speckle and point scatterers using an 18.5 mm, 96 element, 4 MHz transducer: (a) DAS (b) MV ($L = 16$, $K = 0$), (c) MV ($L = 32$, $K = 0$) (d) MV ($L = 48$, $K = 0$).

shows MV using $L = 48$ and different values of K. We see that as the amount of temporal averaging increases, the resolution of the system remains (approximately) the same, but the intensity of the speckle approaches that of DAS. This can also be seen in Fig. 5 which shows the speckle statistics for DAS and MV using the same parameters. As K increases, the average magnitude increases, and the distribution approaches that of DAS.

C. Heart phantom

We applied the DAS and MV beamformers to experimental RF data from a heart phantom. The data were obtained from the Biomedical Ultrasound Laboratory, University of Michigan.[1] The RF data were recorded with a 64 element, 3.33 MHz transducer. All transmitter and receiver combinations were available, and we synthesized fixed transmit focus at 60 mm. Fig. 1 and Fig. 6 shows the images obtained with DAS and MV for different amount of temporal averaging. Both MV results use $L = 32$. The MV image in Fig. 1(b), in which $K = 0$, displays a better definition of the ventricular walls than for the DAS in Fig. 1(a), but the tissue appears less homogeneous and the average intensity of the speckle is lower. This results in an image with lower contrast. The

[1]Ultrasound RF data-set 'heart' from the Biomedical Ultrasound Laboratory, University of Michigan. Available at http://bul.eecs.umich.edu/, April 2006.

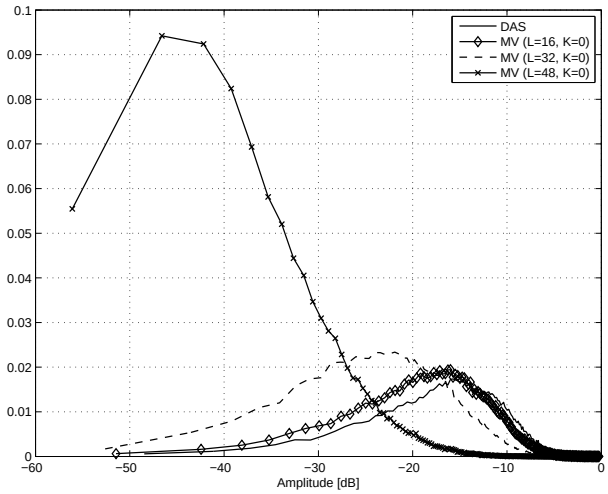

Fig. 3. Magnitude distributions for the speckle in Fig. 2.

MV image in Fig. 6, in which $K = 11$, displays similar resolution as for $K = 0$, but the intensity of the speckle is closer to DAS. Thus, resolution is improved while the contrast is retained.

IV. Discussion

The spatially averaged MV results in Fig. 2 show that we achieve increased resolution when subarray length increases. However, increasing L has a significant effect on speckle: From Fig. 3 we see that the average magnitude of the speckle is reduced by approximately 8 dB for $L = 32$ and approximately 30 dB for $L = 48$ compared to DAS.

Fig. 4 shows that by using temporal as well as spatial averaging, the average magnitude of the speckle approaches that of DAS as K increases. At the same time we retain the the good resolution of Fig. 2(d). From Fig. 5 we see that for $K = 5$, 11 and 22, which corresponds to temporal averaging over 1/2, 1 and 2 pulse lengths, the average speckle magnitude is approximately 10, 4 and 2 dB lower than for DAS, respectively. This shows that similar speckle brightness as DAS is achievable while improving the spatial resolution of the system.

Although the period over which the transmit pulses in medical ultrasound can be considered stationary is short, these results suggest that the one-sample MV beamformers ($K = 0$) do not capture the statistics of a speckle process. The transmit pulse merely acts as a filter on a random, stationary process, forcing use of temporal averaging to capture the spatial covariance of the backscattered signals. While giving an acceptable estimate of the spatial covariance of echoes from strong, isolated scatterers, it yields a poor estimate of the more stationary backscatter from homogeneous tissue. However, by use of temporal averaging the speckle intensity in MV images is similar to DAS, while the good resolution of the beamformer is retained.

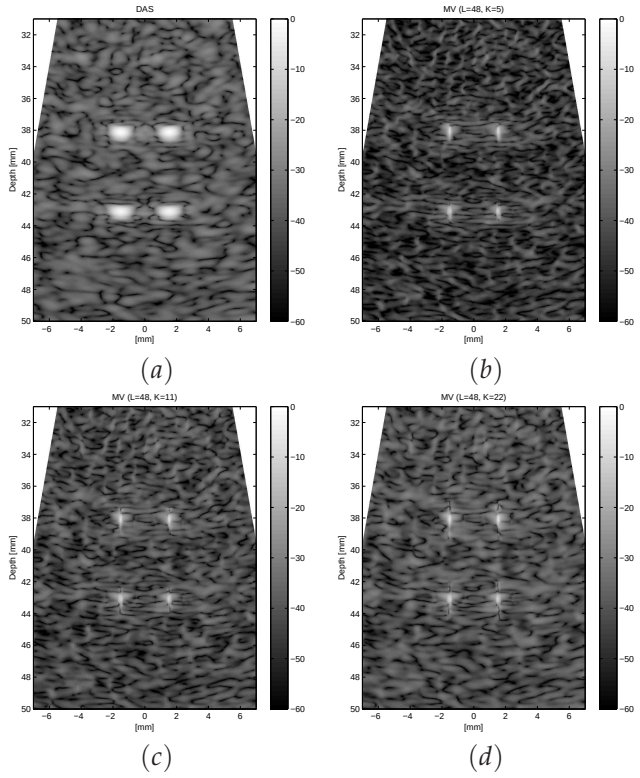

Fig. 4. Images of speckle and point scatterers using an 18.5 mm, 96 element, 4 MHz transducer: (a) DAS (b) MV ($L = 48$, $K = 5$), (c) MV ($L = 48$, $K = 11$) (d) MV ($L = 48$, $K = 22$).

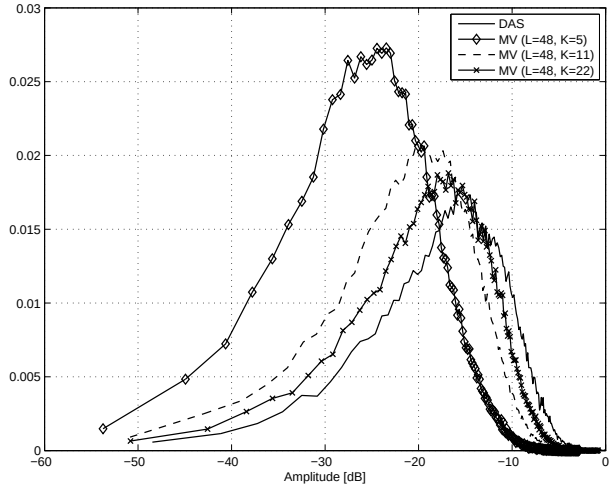

Fig. 5. Magnitude distributions for the speckle in Fig. 4.

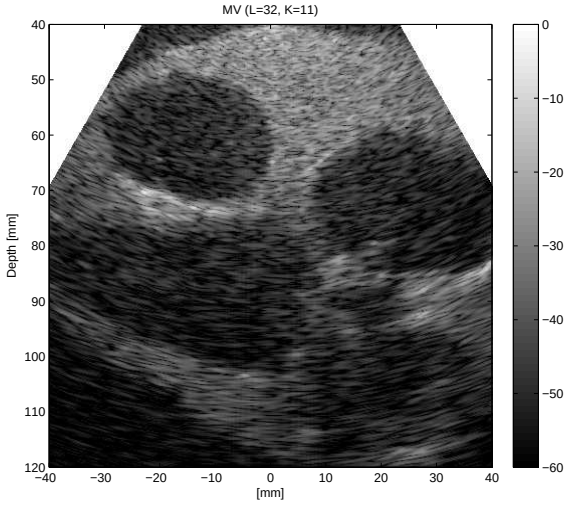

Fig. 6. Heart phantom imaged by a 15.4 mm, 64 element 3.33 MHz transducer using MV beamforming ($L = 32$, $K = 11$). Transmit focus was 60 mm.

V. Conclusion

We have examined the difference in speckle statistics on images formed by delay-and-sum and minimum variance beamformers. We have shown that the differences depend on how the spatial covariance matrix required by the minimum variance beamformer is estimated. By averaging both in the spatial and temporal domain, similar speckle statistics as delay-and-sum is achieved without compromising the improved spatial resolution offered by the minimum variance beamformer.

VI. Acknowledgment

We want to thank Dr Kjell Kristoffersen, GE Vingmed Ultrasound, for pointing out the differences in speckle statistics, and for several helpful discussions.

References

[1] J. A. Mann and W. F. Walker, "A constrained adaptive beamformer for medical ultrasound: Initial results," *Ultrasonics Symposium, 2002. Proceedings. 2002 IEEE*, vol. 2, pp. 1807–1810, October 2002.

[2] M. Sasso and C. Cohen-Bacrie, "Medical ultrasound imaging using the fully adaptive beamformer," *Acoustics, Speech and Signal Processing, 2005. Proceedings (ICASSP '05). IEEE International Conference on*, vol. 2, pp. 489–492, March 2005.

[3] J.-F. Synnevåg, A. Austeng, and S. Holm, "Minimum variance adaptive beamforming applied to medical ultrasound imaging," *Proc. IEEE Ultrasonics Symposium*, vol. 2, pp. 1199–1202, Sept. 2005.

[4] F. Viola and W. F. Walker, "Adaptive signal processing in medical ultrasound beamforming," *Proc. IEEE Ultrasonics Symposium*, vol. 4, pp. 1980–1983, Sept. 2005.

[5] Z. Wang, J. Li, and R. Wu, "Time-delay- and time-reversal-based robust Capon beamformers for ultrasound imaging," *IEEE Transactions on Medical Imaging*, vol. 24, pp. 1308–1322, Oct. 2005.

[6] J.-F. Synnevåg, A. Austeng, and S. Holm, "Adaptive beamforming applied to medical ultrasound imaging," *IEEE Transactions on Ultrasonics, Ferroelectrics, and Frequency Control*, vol. 54, no. 8, pp. 1606–1613, Aug. 2007.

[7] C. B. Burckhardt, "Speckle in ultrasound b-mode scans," *IEEE Transactions on Sonics and Ultrasonics*, vol. SU-25, pp. 1–6, January 1978.

[8] J. Capon, "High-resolution frequency-wavenumber spectrum analysis," *Proc. IEEE*, vol. 57, pp. 1408–1418, August 1969.

[9] R. F. Wagner, S. W. Smith, J. M. Sandrik, and H. Lopez, "Statistics of speckle in ultrasound b-scans," *IEEE Transactions on Sonics and Ultrasonics*, vol. 30, pp. 156–163, May 1983.

[10] J. A. Jensen, "Field: A program for simulating ultrasound systems," *Medical & Biological Engineering & Computing*, vol. 34, pp. 351–353, 1996.